Eur. Phys. J. D **41**, 355–361 (2007)
DOI: 10.1140/epjd/e2006-00247-3

THE EUROPEAN PHYSICAL JOURNAL D

Spatiotemporal dynamics of Bose-Einstein condensates in moving optical lattices

F. Li[a], W.X. Shu, J.G. Jiang, H.L. Luo, and Z. Ren

Department of Physics, Nanjing University, Nanjing 210008, P.R. China

Received 23 April 2006 / Received in final form 25 July 2006
Published online 15 November 2006 –

Abstract. Spatiotemporal dynamics of Bose-Einstein condensates in moving optical lattices have been studied. For a weak lattice potential, the perturbed correction to the heteroclinic orbit in a repulsive system is constructed. We find the boundedness conditions of the perturbed correction contain the Melnikov chaotic criterion predicting the onset of Smale-horseshoe chaos. The effect of the chemical potential on the spatiotemporal dynamics is numerically investigated. It is revealed that the variance of the chemical potential can lead the systems into chaos. Regulating the intensity of the lattice potential can efficiently suppress the chaos resulting from the variance of the chemical potential. And then the effect of the phenomenological dissipation is considered. Numerical calculation reveals that the chaos in the dissipative system can be suppressed by adjusting the chemical potential and the intensity of the lattice potential.

PACS. 03.75.Lm Tunneling, Josephson effect, Bose-Einstein condensates in periodic potentials, solitons, vortices, and topological excitations – 03.75.Kk Dynamic properties of condensates; collective and hydrodynamic excitations, superfluid flow – 05.45.Ac Low-dimensional chaos – 05.45.Gg Control of chaos, applications of chaos

1 Introduction

Ever since Bose-Einstein condensate was first observed in 1995 in experiments at very low temperature [1,2], theoretical and experimental research results on this field have been reported explosively. Among these research works, Bose-Einstein condensates in optical lattices attract more and more interest due to their convenience in studying the dynamical behavior of coherent matter in periodic potentials. The optical lattice can be created by the interference of two or more laser beams [3]. In 1996, Damhan et al. successfully loaded Bose-Einstein condensates in optical lattices [4], and then in 1998 Anderson et al. also realized a similar experiment [5]. From then on, a series of interesting physical phenomena concerning static or moving optical lattices are experimentally and theoretically investigated, such as quantum phase effects [5,6], quantum computation and quantum information [7,8], Bloch oscillations [9], matter-wave transport [10], Landau-Zener tunneling [5,11–14], acceleration of the condensate ground state [10,15–19], chaos [20,21], and the response of a BEC to a weak moving optical potential [22]. In 2002, Denschlag et al. further delivered a series of experimental results with BECs in moving optical lattices [23]. In 2003, Mellish et al. presented a scheme for nonadiabatic loading of a BEC into the ground state of a weak moving optical lattice [24] and Fallani and coworkers reported a lensing effect on a Bose-Einstein condensate expanding in a moving 1D optical lattice [25]. However, due to the abundant dynamical properties of BECs systems in optical lattices, there still exist many open problems to be investigated.

In this paper we study the spatiotemporal dynamics of Bose-Einstein condensates in moving optical lattices. In Section 2, we consider the nondissipative system. By using the direct perturbation technique, we reach a 1st-order corrected chaotic solution whose boundedness conditions contain Melnikov chaotic criterion predicting the onset of Smale-horseshoe chaos. In the light of Melnikov-function method, the condition for the emergence of the heteroclinic chaos is obtained. By using the chaotic solution, we analytically illustrate the incomputability and unpredictability of the system's chaotic evolution of the atom density. The effect of the chemical potential on the spatiotemporal dynamics of the systems is numerically investigated. It is revealed that the variance of the chemical potential can lead the systems into chaos which can be suppressed by regulating the intensity of the lattice potential. In Section 3, the effect of the phenomenological dissipation is considered. We analytically obtain the Melnikov chaotic criterion and numerically find that the chaos in the dissipative system can be suppressed by adjusting the intensities of the chemical potential and the lattice potential. Studies in this paper are based on the nonlinear Schrödinger equation (GP equation), therefore, Hai et al.

[a] e-mail: wiselfhhy@gmail.com

call the chaos of macroscopic wave function macroscopic quantum chaos [26]. In Section 4, we give a summary and some discussions.

2 The nondissipative system

The macroscopic quantum wave function $\Psi(x,t)$ characterizing the dynamical evolution of the BEC system near-zero temperature satisfies the mean-field Gross-Pitaevskii equation [27,28]

$$i\hbar\frac{\partial\Psi}{\partial t} = -\frac{\hbar^2}{2m}\frac{\partial^2\Psi}{\partial x^2} + V_{ext}\Psi + g|\Psi|^2\Psi - \mu\Psi \tag{1}$$

with $\hbar$ being Plank's constant, m the atomic mass, μ the chemical potential and usually a function of the temperature and the total number of condensate atoms, $g = 4\pi a_s\hbar^2/m$ the nonlinearity parameter that takes in account the mean field produced by the other bosons, and a_s the s-wave scattering length. $a_s > 0$ indicates a repulsive interaction and $a_s < 0$ corresponds to an attractive case. Experiment physicists have successfully developed advanced experimental techniques that make it possible to rapidly and effectively adjust the value and sign of the s-wave scattering length by using magnetic-field-induced Feshbach resonance [29]. In this paper, we consider the case that the external confining potential V_{ext} has the form

$$V_{ext} = -\hbar\frac{\Omega_1(t)\Omega_2(t)}{2\Delta}[1-\cos(2kx+\delta t)],$$

which consists of two counter-propagating laser beams along the x-direction. Here, k is the laser wave vector fixing the velocity of the moving laser potential as $v = \delta/(2k)$, δ is the frequency difference between the two laser beams, $\Omega_1(t)$ and $\Omega_2(t)$ are the Rabi frequencies, and Δ is the detuning from resonance. We consider the case with $\Omega_1(t) = \Omega_2(t) = \Omega_0$. So the confining potential becomes $V_{ext} = -I[1-\cos(2kx+\delta t)]$ with $I = \hbar\Omega_0^2/(2\Delta)$ being a constant. In the present work, we take a similar choice to that in [30] by neglecting the constant term. And then the confining potential is reduced to a simple form as $V_{ext} = I\cos(2kx+\delta t)$. So we have the following GP equation

$$i\hbar\frac{\partial\Psi}{\partial t} = -\frac{\hbar^2}{2m}\frac{\partial^2\Psi}{\partial x^2} + I\cos(2kx+\delta t)\Psi + g|\Psi|^2\Psi - \mu\Psi. \tag{2}$$

Traveling wave solutions of GPE have been proved to be effective forms in exploring BEC systems [31–33]. In the present work, because the condensate moves with the moving lattice potential, we also concentrate our attention on the traveling wave solution of the GP equation and set it as

$$\Psi = \phi(\xi)\exp[i(\alpha x+\beta t)] \tag{3}$$

with α and β being two unfixed real parameters. Here, we define a space-time variable $\xi = x + vt$ which shows the traveling wave moves with the same velocity as that of the optical lattice. Solution (3) indicates that the matter wave in the BEC system is a Bloch-like wave.

Substituting equation (3) into equation (2), we obtain an ordinary differential equation

$$\frac{\hbar^2}{2m}\frac{d^2\phi}{d\xi^2} + i\left(\frac{\hbar^2\alpha}{m}+\hbar v\right)\frac{d\phi}{d\xi} - \left(\hbar\beta + \frac{\hbar^2\alpha^2}{2m}\right)\phi - g|\phi|^2\phi = -\mu\phi + I\cos(2kx+\delta t)\phi. \tag{4}$$

It is more convenient to rescale equation (4) through introducing the dimensionless variables

$$\zeta = k\xi, \quad \tilde{v} = 2mv/\hbar k, \quad \tilde{\beta} = \hbar\beta/E_r,$$
$$\tilde{\alpha} = \alpha/k, \quad \tilde{I} = I/E_r, \quad \tilde{\mu} = \mu/E_r, \quad E_r = (\hbar^2k^2)/(2m). \tag{5}$$

Here, $E_r = \hbar^2k^2/2m$ is the recoil energy and we regard $I = \hbar\Omega_0^2/2\Delta$ as the intensity of the optical potential. Then equation (4) can be rewritten as

$$\frac{d^2\phi}{d\zeta^2} + i(2\tilde{\alpha}+\tilde{v})\frac{d\phi}{d\zeta} - (\tilde{\beta}+\tilde{\alpha}^2)\phi - \tilde{g}|\phi|^2\phi = -\tilde{\mu}\phi + \tilde{I}\cos(2\zeta)\phi, \tag{6}$$

where the function ϕ has been normalized in units of the wave vector k and the dimensionless nonlinear interaction coefficient $\tilde{g} = 8\pi a_s k$. Considering the form of equation (6), we assume the function $\phi = A(\zeta)\exp[iB(\zeta)]$, so the total number of atoms in the condensate $N = \int_{-\infty}^{+\infty}|A(\zeta)|^2d\zeta$. Inserting $\phi = A(\zeta)\exp[iB(\zeta)]$ into equation (6) leads equation (6) to

$$\frac{d^2A}{d\zeta^2} - A\left(\frac{dB}{d\zeta}\right)^2 - (2\tilde{\alpha}+\tilde{v})A\frac{dB}{d\zeta} - (\tilde{\beta}+\tilde{\alpha}^2)A - \tilde{g}A^3 + i\left[A\frac{d^2B}{d\zeta^2} + 2\frac{dA}{d\zeta}\frac{dB}{d\zeta} + (2\tilde{\alpha}+\tilde{v})\frac{dA}{d\zeta}\right] = -\tilde{\mu}A + \tilde{I}\cos(2\zeta)A. \tag{7}$$

From equation (7) one can see that the system's dynamical behavior is complex. For simplicity, we consider the case of eliminating the imaginary part of equation (7). To this end, we set

$$2\frac{dA}{d\zeta}\frac{dB}{d\zeta} + (2\tilde{\alpha}+\tilde{v})\frac{dA}{d\zeta} = 0,$$

which leads to $dB/d\zeta = -(\tilde{v}/2+\tilde{\alpha})$ and $d^2B/d\zeta^2 = 0$. Accordingly, equation (7) is reduced to a simple form

$$\frac{d^2A}{d\zeta^2} + \left(\tilde{\mu} - \frac{\tilde{v}^2}{4}\right)A - \tilde{g}A^3 - \tilde{I}\cos(2\zeta)A = 0. \tag{8}$$

In general, the chemical potential $\tilde{\mu}$ is usually a function of the temperature and the total number of condensate atoms. In a practical system both of them are changeable. Meanwhile, the velocity $\tilde{v}$ of the lattice can be effectively adjusted by well and truly regulating k and δ. Therefore, through adjusting experimental facilities and conditions

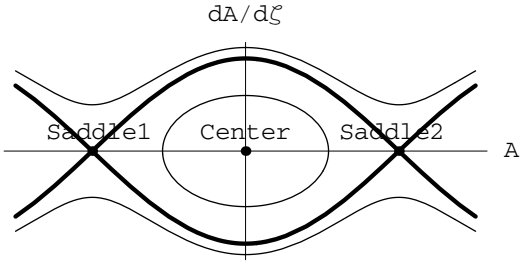

Fig. 1. Phase portrait of the unperturbed system with a center $(A, \dot{A}) = (0, 0)$ and two saddles $(A, \dot{A}) = (\pm\Lambda/\sqrt{\tilde{g}}, 0)$.

there are three choices of the value of $(\tilde{\mu} - \tilde{v}^2/4)$ as expressed below

$$\tilde{\mu} - \frac{\tilde{v}^2}{4} \begin{cases} < 0 \\ = 0 \\ > 0 \end{cases}. \tag{9}$$

And it has been known that the value and sign of the nonlinearity parameter $\tilde{g}$ can also be effectively changed through the Feshbach resonance [29]. Thus, the two following inequalities $\tilde{g} < 0$ and $\tilde{g} > 0$ can be satisfied. When $\tilde{g} = 0$, the system becomes an ideal cloud of noninteracting bosons.

In our perturbation analysis we concentrate our attention on a repulsive system $(\tilde{g} > 0)$ with $(\tilde{\mu} - \tilde{v}^2/4) > 0$. When the laser potential is weak, we can treat it as a perturbation to the system. Accordingly, equation (8) can be rewritten as

$$\frac{d^2A}{d\zeta^2} + \Lambda^2 A - \tilde{g}A^3 = \tilde{I}\cos(2\zeta)A \tag{10}$$

with $\Lambda^2 = \tilde{\mu} - \tilde{v}^2/4$. As is known, equation (10) (also called Duffing equation) describes a periodically driven Duffing oscillator. The Duffing oscillator has always been used as a classical model for analysis of nonlinear phenomena and its dynamical behavior has been widely studied. We can apply direct perturbation and Melnikov-function methods to investigate the chaotic dynamical behavior of the amplitude of the macroscopic quantum wave function. To this aim, first, by assuming $\tilde{I} = 0$ we arrive at an unperturbed Hamiltonian

$$H(A, \dot{A}) = \frac{\dot{A}^2}{2} + \frac{\Lambda^2 A^2}{2} - \frac{\tilde{g}A^4}{4}. \tag{11}$$

And then, in Figure 1 we plot the phase portrait of the unperturbed system. It is demonstrated that there exists one center $(A, \dot{A}) = (0, 0)$ and two saddles $(A, \dot{A}) = (\pm\Lambda/\sqrt{\tilde{g}}, 0)$ in the system. The two orbits passing the saddles are just the heteroclinic orbits forming the separatrix, which is of particular importance in our theoretic analysis. What we are interested in is the system's dynamical behavior close to the separatrix.

Now we expand equation (10)'s solution close to the separatrix as follows

$$A = A_0 + A_1, \quad \text{for } |A_1| \ll |A_0|. \tag{12}$$

Substituting equation (12) into equation (10), we obtain the following equations

$$\frac{d^2A_0}{d\zeta^2} + \Lambda^2 A_0 - \tilde{g}A_0^3 = 0 \tag{13}$$

and

$$\frac{d^2A_1}{d\zeta^2} + \Lambda^2 A_1 - 3\tilde{g}A_0^2 A_1 = \varepsilon_1,$$
$$\varepsilon_1 = \tilde{I}\cos(2\zeta)A_0. \tag{14}$$

From equations (11) and (13), it can be seen that the separatrix solution is just the heteroclinic solution of equation (11) expressed as

$$A_0 = \frac{\Lambda}{\sqrt{\tilde{g}}}\tanh\left[\frac{\Lambda}{\sqrt{2}}(\zeta - \zeta_0)\right] \tag{15}$$

with constant $\zeta_0 = -\sqrt{2}/\Lambda \tanh^{-1}[A_0(0)\sqrt{\tilde{g}}/\Lambda]$.

According to references [26,34–37], when $\varepsilon_1 = 0$, by using the solution of the zeroth order equation one can easily get two linearly independent solutions of equation (14) bearing the following forms

$$f_1 = \frac{dA_0}{d\zeta} = \frac{\Lambda^2}{\sqrt{2\tilde{g}}}\mathrm{sech}^2\left[\frac{\Lambda}{\sqrt{2}}(\zeta - \zeta_0)\right], \tag{16}$$

$$\begin{aligned} f_2 &= \frac{dA_0}{d\zeta}\int\left(\frac{dA_0}{d\zeta}\right)^{-2}d\zeta \\ &= \frac{\sqrt{\tilde{g}}}{\Lambda^2}\mathrm{sech}^2\left[\frac{\Lambda}{\sqrt{2}}(\zeta - \zeta_0)\right]\left\{\frac{3}{4\sqrt{2}}(\zeta - \zeta_0)\right. \\ &\quad + \frac{1}{2\Lambda}\sinh[\sqrt{2}\Lambda(\zeta - \zeta_0)] \\ &\quad \left. + \frac{1}{16\Lambda}\sinh[2\sqrt{2}\Lambda(\zeta - \zeta_0)]\right\}. \end{aligned} \tag{17}$$

Evidently, f_2 is unbounded and will exponentially increase with the growth of ζ due to its inclusion of hyperbolic sine functions. Now, given equations (16) and (17) and through variation of constants, we can easily construct the general solution of equation (14) [26,34–37]

$$A_1 = f_2\int_{C_1}^{\zeta} f_1\varepsilon_1 d\zeta - f_1\int_{C_2}^{\zeta} f_2\varepsilon_1 d\zeta \tag{18}$$

with C_1 and C_2 being two arbitrary constants adjusted by the initial conditions. Applying equations (14), (16) and (17) to equation (18) and carefully calculating the limits for $\zeta \to \infty$ reveal that

$$\lim_{\zeta\to\pm\infty} A_1 \to \pm\infty. \tag{19}$$

Equation (19) indicates that the solution $A_1(\zeta)$ is unbounded thanks to the exponential increasing of f_2 to infinity as $\zeta \to \pm\infty$. This usually means the solution (18) is Lyapunov unstable [37]. However, it is fortunate that the

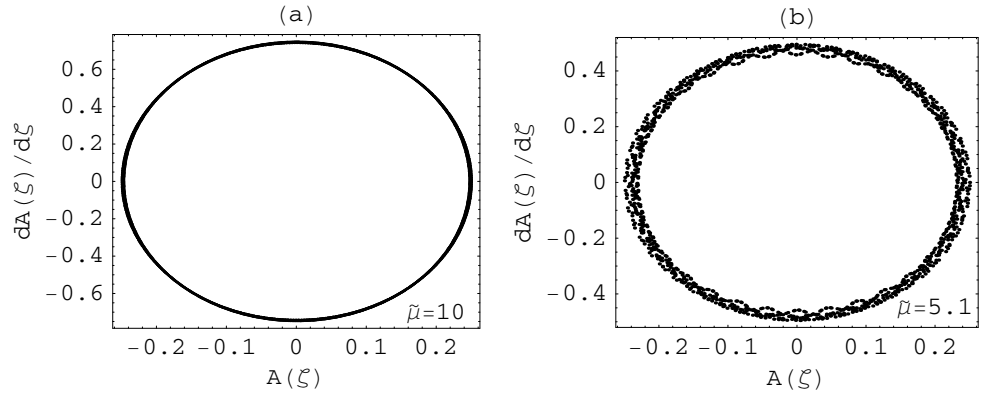

Fig. 2. The phase portraits in $(A, \dot{A})$ plain for repulsive interaction. Figure (a) indicates that the system is in a regular and periodic state. Figure (b) shows that the system is in a non-periodic state. The parameters and initial conditions are set as $\tilde{v} = 2.0, \tilde{I} = 0.25, \tilde{g} = 0.712, A(0) = 0.25$, and $\dot{A} = 0$.

instability can be controlled by some necessary and sufficient conditions, namely, solution (18) can be Lyapunov stable if and only if the following conditions

$$G_{\pm} = \lim_{\zeta \to \pm\infty} \int_{C_1}^{\zeta} f_1 \varepsilon_1 d\zeta = 0 \tag{20}$$

are satisfied [37]. From $G_+ - G_- = 0$, we can eliminate the constant C_1 and subsequently reach

$$M(\zeta_0) = G_+ - G_- = \int_{-\infty}^{+\infty} f_1 \varepsilon_1 d\zeta = 0. \tag{21}$$

To our knowledge, the function $M(\zeta_0)$ is just the well-known Melnikov function

$$M(\zeta_0) = \sin(2\zeta_0)\mathrm{csch}\left(\frac{\sqrt{2}\pi}{\sqrt{\tilde{\mu} - \tilde{v}^2/4}}\right) = 0. \tag{22}$$

Melnikov function is also called Melnikov distance between the stable and unstable manifolds in the Poincaré section at ζ_0. It's well-known that if the Melnikov function $M(\zeta_0)$ has simple zeros, there exists Smale-horseshoe chaos in the system. It is clear that only when $\sin(2\zeta_0) = 0$, namely,

$$\zeta_0 = \pm\frac{n\pi}{2} \tag{23}$$

with i being an integer number, can $M(\zeta_0)$ has simple zeros. Chaos may be destructive sometimes; but it can also be desired for other occasions. Through careful choice of the parameters and initial conditions one can satisfy (23) or not. So one can successfully reach a chaotic or nonchaotic situation.

Now, by using the chaotic solution (18), we analytically illustrate the incomputability and unpredictability of the system's chaotic evolution of the atom density. As can be seen in the chaotic solution (18), the first term of it is a product between the exponential increasing function f_2 and an analytically unsolvable integral, which cannot be expressed as finite terms of elementary functions. It is well-known that any computer cannot calculate infinite terms. All functions of infinite terms are treated as functions of finite terms in computers. Therefore, deviations from the exact value are inevitable in course of calculation. Meanwhile, different numerical integration techniques and different integration steps can also result in such deviations. Furthermore, equation (22) relates the system parameters and constants to the irrational number π, so we cannot choose precise values of system parameters and constants. Therefore, we are not able to avoid deviations during the calculation process in computers. Because of the inclusion of f_2 in the product, those deviations will be exponentially amplified to infinity with the increase of ζ. This indicates the chaotic evolution of the atom density is very sensitive to the initial conditions, system parameters, and integration methods. In a word, the chaotic evolution of the atom density is incomputable and unpredictable. That is a crucial characteristic of chaos.

In typical experiments for repulsive atom-atom interaction to date, the relevant parameters are selected by $a_s = 2.65$ nm and $k = 1.07 \times 10^7$ m^{-1} for Na [38]. Accordingly, the dimensionless nonlinearity parameter $\tilde{g} = 0.712$. Denschlag et al. had demonstrated the maximum lattice velocity in experiment can reach 2.1×10^{-1} ms^{-1} [23] with a corresponding maximum dimensionless velocity $\tilde{v} \approx 14.43$. We adopt Denschlag et al.'s lattice velocity $v = 3.0$ cms^{-1} [23] with the corresponding dimensionless velocity $\tilde{v} \approx 2.0$ for the repulsive system.

The chemical potential is of crucial importance in the formation and stability of BECs. Here, we mainly concentrate our attention on the role of the chemical potential in the spatiotemporal dynamics of the system. With a set of parameters and initial conditions, by using equation (8) we plot $dA(\zeta)/d\zeta$ as a function of $A(\zeta)$ in the phase space of $(A(\zeta), dA(\zeta)/d\zeta)$ in Figures 2 and 3. When the chemical potential $\tilde{\mu} = 10$, there is only a single closed orbit in the phase space as shown in Figure 2a. That means no chaos appears in the system. But when the chemical potential $\tilde{\mu}$ is decreased to 5.1, the closeness of the single orbit is destroyed and the points spread randomly in the phase space as shown in Figure 2b, which implies that the system has stepped into a non-periodic state. When the chemical potential $\tilde{\mu}$ is further decreased to 2.11, a typical chaotic attractor appears, see Figure 3a, which denotes that the system has stepped into a chaotic state. Figure 3b is the corresponding chaotic temporal and spatial evolutions of

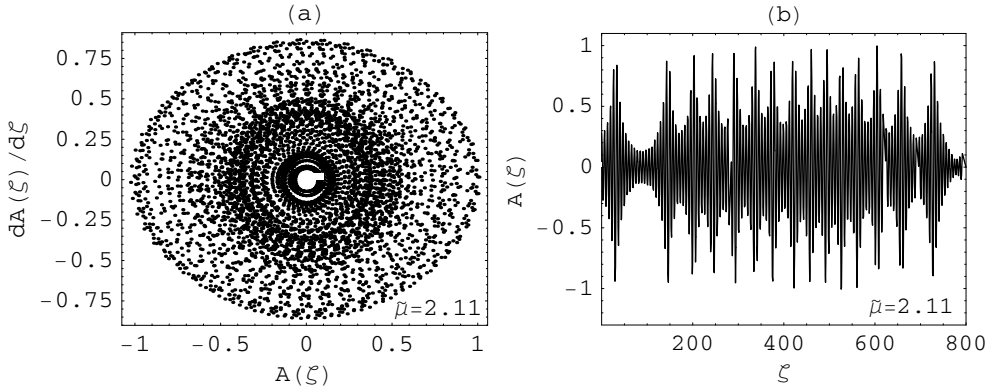

Fig. 3. Figure (a) is a chaotic attractor for the repulsive system in $(A(\zeta), \dot{A}(\zeta))$ plain. Figure (b) is the corresponding temporal and spatial evolutions of $A(\zeta)$ demonstrating that the evolutions of $A(\zeta)$ is chaotic. The parameters and initial conditions are set as those of Figure 2a.

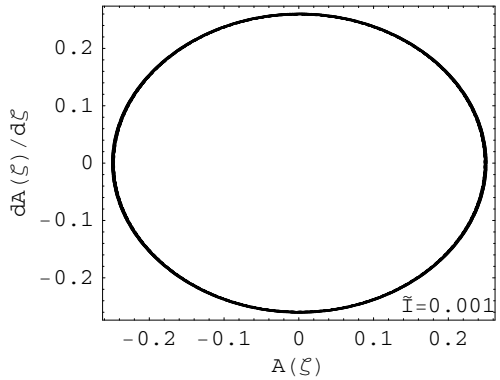

Fig. 4. There is only single closed orbit in the $(A(\zeta), \dot{A}(\zeta))$ plain, which means the chaos have been suppressed. The parameters and initial conditions are the same as those of Figure 3.

$A(\zeta)$. Figures 2 and 3 illuminate that the decrease of the chemical potential can lead the system into a chaotic state.

Fortunately, we numerically find that the chaos can be suppressed by regulating the intensity of the lattice potential.

Suppression of chaos in nonlinear systems is of much practical importance and has received considerable attention in recent years [39]. The growing interest in suppression of chaos comes from the idea of controlling chaos advanced by Ott, Grebogi, and Yorke [40]. Controlling chaos means changing the chaotic motion to regular motion; and then the chaos is suppressed. Braiman et al. had pointed out that chaos in dynamical systems can be controlled with weak periodic perturbations [41]. Here, in the numerical experiment we will demonstrate the suppression of the spatiotemporal chaos in the system by adjusting the intensity of the lattice potential.

Considering the case of Figure 3, we only decrease the intensity of the lattice potential and keep the other parameters fixed. It is found that when the intensity $\tilde{I}$ of the lattice potential is decreased to 0.001, there is only one closed orbit in the phase space, see Figure 4. That is to say, the chaos has been completely suppressed.

3 The dissipative system

In a realistic Quasi-1D system the condensate is prone to damping, e.g., due to a small thermal cloud [42,43]. In order to explore the dissipative dynamics, a damping term $\hbar\lambda\partial\Psi/\partial t$ [44,45] is introduced to the left-hand side of equation (2)

$$(i+\lambda)\hbar\frac{\partial\Psi}{\partial t} = -\frac{\hbar^2}{2m}\frac{\partial^2\Psi}{\partial x^2} + I\cos(2kx+\delta t)\Psi + g|\Psi|^2\Psi - \mu\Psi, \tag{24}$$

here, $\lambda < 0$ for damping. As has been pointed out in reference [45] that the dissipation in the GP equation is treated phenomenologically. This treating way of dissipation follows the work of Choi et al. [44]. But what should be pointed out is that the introduction of damping is only an approximate way of treating thermal dissipation in the system.

Considering the traveling solution expressed as solution (3), we easily get the following ordinary differential equation

$$\frac{\hbar^2}{2m}\frac{d^2\phi}{d\xi^2} + i\left(\frac{\hbar^2\alpha}{m} + \hbar v - i\hbar\lambda v\right)\frac{d\phi}{d\xi} - \left(\hbar\beta + \frac{\hbar^2\alpha^2}{2m} - i\hbar\beta\lambda\right)\phi - g|\phi|^2\phi = -\mu\phi + I\cos(2kx+\delta t)\phi. \tag{25}$$

For simplicity, we apply the dimensionless variables defined in equation (5) to equation (25), and then equation (25) is changed into

$$\frac{d^2\phi}{d\zeta^2} + i(2\tilde{\alpha} + \tilde{v} - i\lambda\tilde{v})\frac{d\phi}{d\zeta} - (\tilde{\beta} + \tilde{\alpha}^2 - i\tilde{\beta}\lambda)\phi - \tilde{g}|\phi|^2\phi = -\tilde{\mu}\phi + \tilde{I}\cos(2\zeta)\phi \tag{26}$$

with the dimensionless nonlinear interaction coefficient $\tilde{g} = 8\pi a_s k$ and the function ϕ being normalized in units of the wave vector k. Like in the above section, assuming $\phi = A(\zeta)\exp[iB(\zeta)]$ and applying it to equation (26)

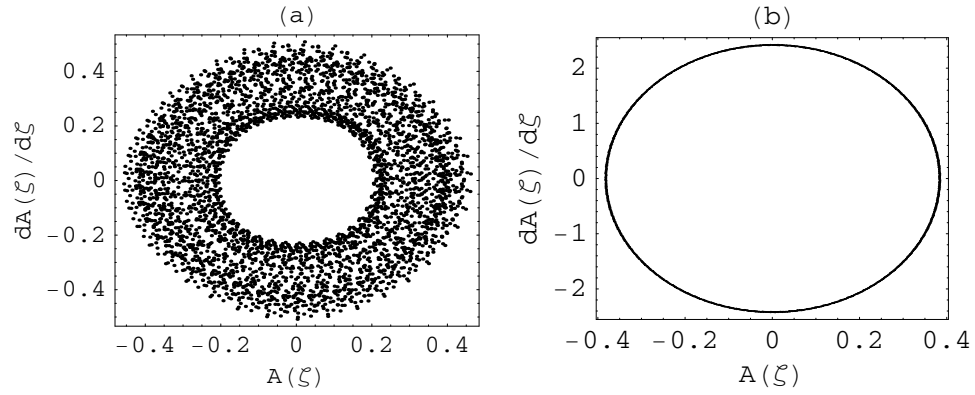

Fig. 5. Phase portraits in the $(A(\zeta), \dot{A}(\zeta))$ plain. Figure (a) is a chaotic attractors with $\tilde{\mu} = 1.28$ and $\tilde{I} = 0.26$. Figure (b) is a periodic attractor with $\tilde{v} = 0.005$ and $\tilde{\mu} = 40$. The other parameters and initial conditions are set as $\tilde{g} = 0.712$, $\tilde{I} = 0.26$, $A(0) = 0.4$, and $dA(\zeta)/d\zeta|_{\zeta=0} = 0$.

lead to

$$\frac{d^2A}{d\zeta^2} - A(\frac{dB}{d\zeta})^2 - (2\tilde{\alpha}+\tilde{v})A\frac{dB}{d\zeta} + \lambda\tilde{v}\frac{dA}{d\zeta} - (\tilde{\beta}+\tilde{\alpha}^2)A - \tilde{g}A^3 + i[A\frac{d^2B}{d\zeta^2} + 2\frac{dA}{d\zeta}\frac{dB}{d\zeta} + (2\tilde{\alpha}+\tilde{v})\frac{dA}{d\zeta} + \lambda\tilde{v}A\frac{dB}{d\zeta} + \lambda\tilde{\beta}A] = -\tilde{\mu}A + \tilde{I}\cos(2\zeta)A. \quad (27)$$

Equation (27) itself demonstrates its extreme complexity. We consider the case of eliminating the imaginary part of equation (27). It is found that when the two conditions

$$2\frac{dA}{d\zeta}\frac{dB}{d\zeta} + (2\tilde{\alpha}+\tilde{v})\frac{dA}{d\zeta} = 0,$$
$$\lambda\tilde{v}A\frac{dB}{d\zeta} + \lambda\tilde{\beta}A = 0,$$

are satisfied, i.e., $dB/d\zeta = -\tilde{\beta}/\tilde{v} = -(\tilde{v}/2 + \tilde{\alpha})$, we can successfully eliminating the imaginary part of equation (27). Accordingly, equation (27) is reduced to the following simple equation

$$\frac{d^2A}{d\zeta^2} + \left(\tilde{\mu} - \frac{\tilde{v}^2}{4}\right)A - \tilde{g}A^3 = \tilde{I}\cos(2\zeta)A + \lambda\tilde{v}\frac{dA}{d\zeta}. \quad (28)$$

When the damping and the lattice potential are so weak that they can be treated as perturbations to the system, the Melnikov function for the system governed by equation (28) is

$$\Delta M(\zeta_0) = -\frac{4\pi\tilde{I}}{\tilde{g}}\sin(2\zeta_0)\mathrm{csch}\left(\frac{\sqrt{2}\pi}{\sqrt{\tilde{\mu}-\tilde{v}^2/4}}\right) + \frac{2\sqrt{2}}{3\tilde{g}}\lambda\tilde{v}\left(\tilde{\mu}-\frac{\tilde{v}^2}{4}\right)^{3/2} = 0. \quad (29)$$

with constant $\zeta_0 = -\sqrt{2}/\Lambda\tanh^{-1}[A_0(0)\sqrt{\tilde{g}}/\Lambda]$.

To guarantee the Melnikov function $\Delta M(\zeta_0)$ has simple zeros, the following equation

$$\frac{d\Delta M}{d\zeta_0} = -\frac{8\pi\tilde{I}}{\tilde{g}}\cos(2\zeta_0)\mathrm{csch}\left(\frac{\sqrt{2}\pi}{\sqrt{\tilde{\mu}-\tilde{v}^2/4}}\right) \neq 0 \quad (30)$$

must be satisfied, namely, $\cos(2\zeta_0) \neq 0$, which results in $\sin(2\zeta_0) \neq \pm 1$. Combining this with equation (29), we get the relationship between the parameters of the chaotic region as follows:

$$\left|\frac{\sqrt{2}\lambda\tilde{v}(\tilde{\mu}-\tilde{v}^2/4)^{3/2}}{6\pi\tilde{I}}\sinh\left(\frac{\sqrt{2}\pi}{\sqrt{\tilde{\mu}-\tilde{v}^2/4}}\right)\right| < 1. \quad (31)$$

According to equation (31), it is obvious that, through adjusting the frequency difference δ between the two laser beams, the laser wave vector k, the detuning Δ, and the Rabi frequency Ω_0, one can keep the values of parameters away from or in the parameter space determined by equation (31) in experiments. In other words, the inequality (31) is experimentally reachable.

Because the introduction of damping is only an approximate way of treating the dissipation, one cannot completely rely on this for discussion of chaos in such systems.

In order to see clearly the dynamical properties of the dissipative system, with a set of parameters and initial conditions we numerically solve equation (28) and plot Figure 5. We adopt the value of $\lambda = -0.03$ determined by Choi et al. in their work [44]. From Figure 5a one can see a typical chaotic attractor in the phase space. But when $\tilde{v} = 0.005$ and $\tilde{\mu} = 40$ and the other parameters are kept unchanged, we find the chaos disappears and there is only one closed orbit in the phase space as shown in Figure 5b. This implies that the chaos is suppressed.

4 Summary and discussions

In summary, we have investigated the spatiotemporal dynamics of Bose-Einstein condensates in moving optical lattices. We use direct perturbation and Melnikov-function methods to theoretically study the space-time chaos in the presence of repulsive atom-atom interaction. The condition for the emergence of the heteroclinic chaos is obtained. Through the first order corrected solution, we analytically demonstrate the incomputability and unpredictability of space-time evolution of the atom density. It is numerically revealed that the variance of the chemical potential can lead the system into chaos. But, regulating the intensity of the lattice potential can efficiently suppress the chaos resulting from the variance of the chemical

potential. In a realistic quasi-1D system the condensate is usually prone to damping, therefore, the effect of the phenomenological dissipation is considered. The Melnikov chaotic criterion for the dissipative system is analytically obtained. Numerical calculation reveals that the chaos in the dissipative system can be suppressed by adjusting the chemical potential and the intensity of the lattice potential.

One thing to be clarify is that the conclusions are correct for the two particular situations, where the governing equations imply that the results provide an indicative behavior (chaos) of such a system. Another thing which we want to point out is that if the relation $\tilde{\mu} - \tilde{v}^2/4 > 0$ cannot be satisfied, chaos can also exist in some parameter regions.

Denschlag and co-workers had successfully loaded Bose-Einstein condensates into optical lattices. If the parameters and initial conditions satisfy the chaotic criterion, chaos can be observed.

To our knowledge, the stability of the condensates is of great importance in dynamic manipulation, quantum computation, quantum information processing, and so on. However, chaos in BEC systems can undermine the stability. Hence, studies on chaos in BEC systems are important.

This work is supported by the National Natural Science Foundations of China (10125521 and 10535010), the 973 National Major State Basic Research and Development of China (G200007740), by the CAS Knowledge Innovation Project No. KJCX2-SW-N02 and by the Fund of Education Ministry of China under contract 20010284036.

References

1. M.H. Anderson, J.R. Ensher, M.R. Matthews, C.E. Wieman, E.A. Cornell, Science **269**, 198 (1995)
2. K.B. Davis, M.-O. Mewes, M.R. Andrews, N.J. van Druten, D.S. Durfee, D.M. Kurn, W. Ketterle, Phys. Rev. Lett. **75**, 3969 (1995)
3. N.K. Efremidis, S. Sears, D.N. Christodoulides, J.W. Fleischer, M. Segev, Phys. Rev. E **66**, 046602 (2002)
4. M. BenDahan, E. Peik, J. Reichel, Y. Castin, C. Salomon, Phys. Rev. Lett. **76**, 4508 (1996)
5. B.P. Anderson, M.A. Kasevich, Science **282**, 1686 (1998)
6. S. Liu, H. Xiong, Z. Xu, G. Huang, J. Phys. B **36**, 2083 (2003)
7. J.K. Pachos, P.L. Knight, Phys. Rev. Lett. **91**, 107902 (2003)
8. R. Ionicioiu, P. Zanardi, Phys. Rev. A **66**, 050301(R) (2002)
9. O. Morsch, J.H. Müller, M. Cristiani, D. Ciampini, E. Arimondo, Phys. Rev. Lett. **87**, 140402 (2001)
10. D.I. Choi, Q. Niu, Phys. Rev. Lett. **82**, 2022 (1999)
11. B. Wu, Q. Niu, Phys. Rev. A **64**, 061603(R) (2001)
12. M. Cristiani, O. Morsch, J.H. Müller, D. Ciampini, E. Arimondo, Phys. Rev. A **65**, 063612 (2002)
13. J. Liu et al., Phys. Rev. A **66**, 023404 (2002)
14. D.I. Choi, Q. Niu, Phys. Lett. A **318**, 558 (2003)
15. A. Trombettoni, A. Smerzi, Phys. Rev. Lett. **86**, 2353 (2001)
16. K. Berg-Sørensen, K. Mølmer, Phys. Rev. A **58**, 1480 (1998)
17. M. Holthaus, J. Opt. B: Quant. Semiclass. Opt. **2**, 589 (2000)
18. M.M. Cerimele, M.L. Chiofalo, F. Pistella, S. Succi, M.P. Tosi, Phys. Rev. E **62**, 1382 (2000)
19. R.G. Scott, A.M. Martin, T.M. Fromhold, S. Bujkiewicz, F.W. Sheard, M. Leadbeater, Phys. Rev. Lett. **90**, 110404 (2003)
20. G. Chong, W. Hai, Q. Xie, Chaos **14**, 217 (2004)
21. G. Chong, W. Hai, Q. Xie, Phys. Rev. E **71**, 016202 (2005)
22. P.A. Ruprecht, M. Edwards, K. Burnett, C.W. Clark, Phys. Rev. A **54**, 4178 (1996)
23. J.H. Denschlag et al., J. Phys. B **35**, 3095 (2002)
24. A.S. Mellish, G. Duffy, C. McKenzie, R. Geursen, A.C. Wilson, Phys. Rev. A **68**, 051601(R) (2003)
25. L. Fallani, F.S. Cataliotti, J. Catani, C. Fort, M. Modugno, M. Zawada, M. Inguscio, Phys. Rev. Lett. **91**, 240405 (2003)
26. W. Hai, C. Lee, G. Chong, L. Shi, Phys. Rev. E **66**, 026202 (2002)
27. N.G. Parker, N.P. Proukakis, C.F. Barenghi, C.S. Adams, Phys. Rev. Lett. **92**, 160403 (2004); N.G. Parker, N.P. Proukakis, C.F. Barenghi, C.S. Adams, J. Phys. B **37**, S175 (2004)
28. N.P. Proukakis, N.G. Parker, C.F. Barenghi, C.S. Adams, Phys. Rev. Lett. **93**, 130408 (2004)
29. Y. Kagan, E.L. Surkov, G.V. Shlyapnikov, Phys. Rev. Lett. **79**, 2604 (1997); S.L. Cornish, N.R. Claussen, J.L. Roberts, E.A. Cornell, C.E. Wieman, Phys. Rev. Lett. **85**, 1795 (2000)
30. M. Machholm, C.J. Pethick, H. Smith, Phys. Rev. A **67**, 053613 (2003)
31. E.V. Goldstein, P. Meystre, Phys. Rev. A **59**, 1509 (1999)
32. E.V. Goldstein, P. Meystre, Phys. Rev. A **59**, 3896 (1999)
33. H.Y. Ling, Phys. Rev. A **65**, 013608 (2001)
34. Q. Xie, W. Hai, G. Chong, Chaos **13**, 801 (2003); G. Chong, W. Hai, Q. Xie, Chaos **14**, 217 (2004)
35. F. Li, W. Hai, Acta Phys. Sin. **53**, 1309 (2004); F. Li, W. Hai, G. Chong, Q. Xie, Commun. Theor. Phys. **42**, 599 (2004)
36. F. Li, W. Hai, Z. Ren, W. Shu, Phys. Lett. A **355**, 104 (2006)
37. W. Hai, Y. Duan, X. Zhu, X. Luo, L. Shi, J. Phys. A **31**, 2991 (1998)
38. S. Inouye et al., Nature **392**, 151 (1998)
39. S.T. Vohra et al., Phys. Rev. Lett. **75**, 65 (1995); K. Taniguchi, Y. Kawai, Phys. Rev. Lett. **83**, 548 (1999); C.U. Choe et al., Phys. Rev. E **72**, 036206 (2005)
40. E. Ott, C. Grebogi, J. Yorke, Phys. Rev. Lett. **64**, 1196 (1990)
41. Y. Braiman, I. Goldhirsch, Phys. Rev. Lett. **66**, 2545 (1991); R. Chacón, J.D. Bejarano, Phys. Rev. Lett. **71**, 3103 (1993)
42. P.O. Fedichev et al., Phys. Rev. A **60**, 3220 (1999)
43. A. Muryshev et al., Phys. Rev. Lett. **89**, 110401 (2002)
44. S. Choi, S.A. Morgan, K. Burnett, Phys. Rev. A **57**, 4057 (1998)
45. K. Kasamatsu, M. Tsubota, M. Ueda, Phys. Rev. A **67**, 033610 (2003)